Mechanism of the solvent-free reactions between indole derivatives and 4-nitrobenzaldehyde studied by solid-state NMR and DFT calculations

Mechanism of the solvent-free reactions between indole derivatives and 4-nitrobenzaldehyde studied by solid-state NMR and DFT calculation

Michele R. Chierotti, Katia Gaglioti, Roberto Gobetto,* Margherita Barbero, Carlo Nervi

Department of Chemistry, University of Torino, Via P. Giuria n° 7, I-10125 Torino, Italy

Abstract

In an effort to determine the details of the solid-state reaction mechanism of the Friedel-Crafts hydroxylalkylation between indole derivatives (indole, **1**^{A}, and N-methylindole, **1**^{B}) and an aromatic aldehyde (4-nitrobenzaldehyde) a series of solid-state NMR experiments have been performed. The reaction proceeds through a melted phase. By means of the DE pulse sequence the hydroxylic intermediate species (1H-indol-3-yl)(4-nitrophenyl)methanol (**3**^{A}) and (1-methyl-1H-indol-3-yl)(4-nitrophenyl)methanol (**3**^{B}) in the melt could be observed and characterized providing evidences for elucidating the reaction mechanism. To support the experimental results, DFT calculation have been carried out showing that the first step of the reaction involving indole and nitrobenzaldehyde to give the intermediate **3**^{A} is energetically favored by 24.7 kJ/mol, whereas the final product (3,3'-((4-nitrophenyl) methylene)bis(3a,7a-dihydro-1H-indole)) (**5**^{A})is 54.8 kJ/mol lower in energy than the reactants. The calculated and experimental chemical shifts are also in good agreement providing further support to the proposed mechanism.

Introduction

Solvent-free organic syntheses are gathering increasing interest from the viewpoint of green chemistry.[1]
In recent years, under the impetus of crystal engineering,[2] solvent-free processes have begun to be investigated for the preparation of crystalline materials,[3] molecular cocrystals,[4] coordination networks[5] and salts.[6] Such solvent-free systems have been recently reviewed[7] and variously termed as solid-solid[8] or solid-state reactions.[9]
However, Scott and co-workers have highlighted that often solvent-free reactions actually proceed through formation of eutectic phases between reactants or between reagents and product(s), i.e. through formation of a liquid or melted phase containing an intimate mixture of macroscopic solid reactant particles. In this way molecules of the solid particles are sufficiently mobile for frequent molecular collisions to occur.[10] Thus, these reactions should be classified as liquid/liquid or liquid/solid systems reacting without added solvents as confirmed also by other authors,[11] though each case has to be carefully evaluated and confirmed.
Concerning solid-solid reactivity, there has been great interest in finding mechanistic aspects in the context of intra-and inter-crystal reactions. The crystal packing determines the extent of molecular loosening required for the reactants to reorient sufficiently to undergo molecular changes. In this context Kaupp has put forward a general mechanism involving three stages.[12]
In studies of reacting solid-state systems, information is often required about phases or compounds present, their structure or mechanisms of their formation or decomposition.
Despite recent progresses of the preparative mechanochemistry, understanding of physical and chemical events that take place in solids during mechanical processing remains limited.
Indeed, the absence of solvent usually requires that other means (co-grinding or kneading) have to be used to bring molecules into contact and to activate the formation of specific interactions. As a consequence, crystals tend to shatter into microcrystalline particles as the reaction proceeds, diminishing the usefulness of X-ray diffraction (XRD) methods for the characterization that requires solid-state spectroscopic techniques.[13] Among these, solid-state NMR (SS NMR) spectroscopy plays an important role since it relies on the nuclear local environment rather than the long-range order providing information on reaction proceeding and product formation.
In this work we show how SS NMR is able to follow solvent-free reactions individuating the mechanism through detection of intermediate species and characterization of solid powdered products. Here we report an exploration of solvent free Friedel-Crafts hydroxylalkylation reaction between indoles (indole, **1**^{A}, and N-

methylindole, $\mathbf{1}^{B}$) and an activated aromatic aldehyde (4-nitrobenzaldehyde, **2**) that we were able to follow by a series of solid-state NMR experiments.
This electrophilic aromatic substitution reaction gives rise to bisindolylmethanes and it has been carried out in the presence of a wide number of Brønsted or Lewis acid as catalysts.[14] Recently, we reported a new practical synthesis of a number of triaryl- , bisindolyl- and trisindolylmethanes in solvent-free reaction conditions, at room temperature or under heating, in the presence of a strong Brønsted acid in catalytic amounts.[15] Following this procedure the product yields are ranging 73-100% (19 examples). Furthermore, starting from the strongly activated 4-nitrobenzaldehyde and indoles, the reaction reached completion in the absence of any catalyst, only by heating the reaction mixture for 1 or 2 h (3 examples; 70, 86 and 100% yields).
To the best of our knowledge, Friedel–Crafts hydroxyalkylation reactions without catalyst have been reported only by us and Patil, in neat conditions and under heating, and by Li in glycerol at 90 uC, where the role of the protic solvent in promoting aldehyde activation through hydrogen bonding was considered a plausible explanation.[15] Therefore, according to the literature, it would appear that the reaction does not proceed in a solvent in the absence of a catalyst at room temperature. Carrying out the reaction in a non-protic solvent would require a catalyst. Interested in the reaction mechanism, we decided to investigate further the reaction under solvent-free reaction conditions and in the absence of any catalyst.

Results and Discussion
The reaction between $\mathbf{1}^{A}$ and **2** proceeds through the formation of an eutectic phase melted at temperature below 30°C.
In this case we relied on the SS NMR ability of characterizing both melted and solid phases through different pulse sequences: direct excitation coupled with high power decoupling (DE) and cross polarization (CP), respectively both under magic angle spinning (MAS) conditions. These, in turn, allow to observe intermediate species present in the melt and to characterize the solid product.
Indeed, a melted is very similar to the solution phase where the molecular tumbling provides efficient relaxation mechanisms able to drastically reduce relaxation delays (T_1) and to average the heteronuclear dipolar interactions. This allows the direct acquisition of heteronuclei such as ^{13}C in reasonable times through DE experiments. This technique has been used for studied melted phases reported in literature such as molten salts.[16]
For solid molecules, the lack of mobility leads to ^{13}C T_1 of hours and to strong heteronuclear dipolar interactions. In this case, the CPMAS pulse sequence, expressly built for rigid solids, is very efficient since relies on shorter T_1 of protons whose magnetization is transferred to heteronuclei (for instance ^{13}C) through the heteronuclear dipolar interaction. This allows either a higher scan number to be acquired in time and a signal intensity gain since we transfer magnetization from an abundant high-γ (^{1}H: 100%, $26.7\cdot10^{7}$ rad T^{-1} s^{-1}) to a diluted low-γ (^{13}C: 1.1%, $6.7\cdot10^{7}$ rad T^{-1} s^{-1}) nucleus.
Solid powdered $\mathbf{1}^{A}$ and **2** liquefy almost immediately upon contacting each other without intervention of grinding. Similar behaviors have been already reported for other cases.[17]
The liquefaction is rapid and complete (10 min) and yields an orange liquid phase (figure 1). The reaction takes about 24 hours to complete with the precipitation of a yellow solid product, characterized as $\mathbf{5}^{A}$ (Scheme 1).
Evolution of the melted phase has been followed during time by DE NMR spectra (figure 2 selected spectra, see SI for the complete series of spectra). In order to fully understand the reaction mechanism the reagents have been mixed either in 2:1 and 1:1 $\mathbf{1}^{A}$:**2** ratios. The main discussion will be focus on the reaction with the 2:1 ratio, shown in Figure 2, since also the 1:1 ratio leads to the di-substituted product $\mathbf{5}^{A}$ together with unreacted **2**. This is in agreement with the high reactivity of the carbocation species supposed to be an intermediate (*see below*). The t=0 DE spectrum (the accumulation takes about 30 minutes) (Figure 2a) is characterized by very narrow (solution-like) resonances directly related to the reactant peaks. The assignment of the melted phase, based on reagent spectra (Figure 3, Table 1), is reported in Table 2 (for atom labeling we refer to scheme 1). At t=2h new small signals are observed indicating the formation of intermediate species in the melt (Figure 2b). It is worth noting the decrease of the aldehydic peak at 191.0 ppm (note that chemical shifts of the melt slightly differ from those of solid reagents) with the concomitant appearing of three resonances at 39.7, 68.9 and 78.7 ppm. All signals are associated to CH atoms as

confirmed by the ^{13}C DE spectrum acquired without decoupling (Figure 2e) which shows doublet signals for all these resonances due to ^{1}H-^{13}C scalar couplings (126, 144 and 154 Hz, respectively). The former is attributed to C7 of the final product **5**^{A}, the second to C7 of the hydroxylic intermediate **3**^{A} (scheme 1), while the latter to an unknown intermediate species (*see below*).
After 7 hours, (Figure 2c with inset) all the cited signals increase their intensity and it is easier to distinguish three sets of resonances with similar behaviours: 1) signals at 68.9 (C7=CH), 150.9 (C4=C_q) and 146.2 (C1=C_q); 2) signals at 39.7 (C7=CH), 152.0 (C4=C_q) and 145.5 (C1=C_q) and 3) signals at 78.7 CH, 146.9 C_q, 146.0 (sh) C_q. The first two sets are attributed to **3**^{A} and **5**^{A}, respectively (see Scheme 1). The third set (78.7 CH, 146.9 C_q, 146.0 (sh) C_q) is associated to an unknown intermediate species probably characterized by the presence of a strong hydrogen bond on the OH group able to shift the signal from 68.9 to 78.7 ppm. Likely, this interaction involves also the NH group of another indole molecule. We believe that the formation of this O-H···N contact, possible only with the lack of N-substituents, promotes and catalyzes the reaction. This is confirmed by the longer time required for the reaction carried out with the N-methyl analogue **1**^{B}.
Afterwards, no significant changes are observed in the spectrum (Figure 2d, t=13h) but an increasing of linewidths and noise level are in agreement with reagent consuming and product precipitation. This is confirmed by the disappearing of the aldehydic peak (191.0 ppm) and of all peaks associated to intermediate species and to the final product.
At the end of the reaction (after 24 hours) by switching to CPMAS techniques, the spectrum of the solid product **5**^{A} was acquired (Figure 2f). The signal assignment of **5**^{A} (Table 1) has been done with the help of the non-quaternary-suppression (NQS) technique which shows only quaternary carbon atoms. It also highlights the presence of two independent molecules in the unit cell as easily observed from the splitting of the signals related to atoms C1 (144.8/142.7 ppm), C4 (154.7/151.9 ppm), C7 (39.7/38.9 ppm) and C15 (136.8/136.1 ppm).
It is worth noting that a) the reagent mixture is a melt and thus observable by DE only; b) the product forms quite suddenly but remains in the melt for hours allowing its direct acquisition by DE experiments. Later (after about 13 hours), it precipitates as yellow powdered solid observable only by CPMAS techniques; c) the intermediate species **3**^{A} is a melted phase rather than solid. This has also been confirmed by following the reaction by CPMAS experiments which do not show any signal until the formation of an adequate amount of **5**^{A} (*see below*). However, **3**^{A} is clearly observed by DE experiments; d) the reaction proceeds through **3**^{A} which looses a water molecule leading to the carbocation species **4**^{A} which immediately converts to **5**^{A}. Owing to long NMR acquisition time (about 15 minutes for reliable signal to noise ratio), it was not possible to observe **4** which is known to be a very reactive species.[18]
By following the reaction by CPMAS, after 13 hours it was possible to observe the product spectrum. No signals were found by applying ^{13}C CPMAS techniques acquired in the initial 7-8 hours. Indeed, one has to consider the low NMR sensitivity, the acquisition time required (about 1-2 hours needed for each spectrum), and, most important, that **3**^{A} and **4**^{A} are in the melt, thus not detectable by CPMAS.
Similar analysis has been performed for the reaction between the N-methyl analogue, **1**^{B}, which is liquid at RT, and **2**. As in the previous case, after few minutes a homogeneous liquid phase is formed without grinding. The reaction takes longer (about 48 h) to complete and at the end a yellow solid product, characterized as **5**^{B}, is recovered. Selected NMR spectra are reported in figure 4 together with the DE spectrum acquired without decoupling (t=13h) and the CPMAS spectrum of **5**^{B} (all the spectra are reported in the SI).
The following considerations can be drawn: a) the reaction proceeds through the intermediates **3**^{B} and **4**^{B}. The former is highlighted by the signal at 68.6 ppm, while the latter again is not observable. b) The product, **5**^{B}, appears in the melt (representative resonance at 39.8 ppm) and precipitates at the end of the reaction. However, c) no signal around 78 ppm is observed at any time. Thus, we can conclude that the presence of a methyl group hampers the formation of the hydrogen-bonded intermediate able to catalyze and accelerate the reaction. At t = 9, 11 and 13h the absence of the hydrogen-bonded intermediate and of **5**^{B} allows the complete individuation and assignments of **3**^{B} as reported in Table 2.
Rather long acquisition times prevent an accurate kinetic study so to support the proposed reaction mechanism, DFT calculation in gas phase at B3LYP/6-311++G(d,p) level have been performed. DFT shows that the overall reaction depicted in Scheme 1 is thermodynamically favored. The first step of the reaction involving indole and nitrobenzaldehyde (**1**^{A} and **2**, Scheme 1) to give the intermediate **3**^{A} is energetically

favored by 24.7 kJ/mol, whereas the final product **5**^{A} is 54.8 kJ/mol lower in energy than the reactants. The structure of the intermediate **3**^{A} has been optimized, its absolute NMR shieldings computed and the corresponding chemical shifts compared with the SSNMR experimental data (Table 2). The two computed optical isomers of **3**^{A} have the same energy (minimal differences are due to local minima). During DFT calculations we do not take in account the interactions in the melted phase. Nevertheless the calculated and experimental chemical shifts summarized in Table 2 are in good agreement, and the general trend of the chemical shifts is reasonably well reproduced by the calculations. In particular, the computed resonances of C7 atoms of **3**^{A} and **5**^{A}, 73.5 and 43.5 ppm, fit well with the observed experimental data of 68.9 and 39.8, respectively, which lay in a region of chemical shifts free of other resonances. From Table 2 one can note that the optimized molecular geometry of **5**^{A} is not symmetric, inducing different values of the chemical shifts (show in parentheses) for the two indole atoms that should be magnetically equivalent due to the free rotation around the C–C bonds. The small discrepancies observed between calculated and experimental chemical shifts can be explained by the neglect of the dynamics and the weak interactions in the melted phase, which induces slightly different local energy minima.

Conclusions

We have characterized the mechanism of the solid-state Friedel-Crafts hydroxylalkylation reaction between indole derivatives (indole, **1**^{A}, and N-methylindole, **1**^{B}) and the aromatic 4-nitrobenzaldehyde with unprecedented detail. A combination of solid-state NMR spectroscopy analysis supported by DFT calculation allowed us to detail a reaction mechanism in which the intermediate species **3**^{A} and **3**^{B} were observed and characterized in the melt. A new hydrogen-bonded intermediate species, responsible for the higher reaction rate starting from **1**^{A}, has been detected. The lack of substituent in the nitrogen position in the indole moiety seems to be the reason for the formation of a hydrogen bond with the hydroxyl intermediate **3**. Furthermore, the CPMAS technique allowed the characterization of solid products that, due to solvent-free methods, are hardly obtained as single crystal suitable for the X-ray analysis. In conclusion we have demonstrated that SS NMR techniques represent an excellent opportunity for studying solvent-free reactions which proceed either through melt or solid phases.

Experimental part

All reagents were commercial and used without further purification.

SS NMR spectroscopy. All SS NMR spectra were recorded on a Bruker Avance II 400 instrument operating at 400.23 and 100.65 MHz for ^{1}H and ^{13}C nuclei, respectively.

For monitoring the evolution of intermediate species in the melt, 1:1 mixtures of reagents were put inside 4 mm rotors in a disposable Kel-F insert sealed with glue. Direct excitation (DE) experiments were acquired with a ^{1}H 90° pulse of 5 μs, recycle delays of 5 s and 350 transients. When applied, the two pulse phase modulation (TPPM) decoupling scheme was used with a frequency field of 75 kHz.

Solid reagent and product samples were packed in cylindrical 4 mm (o.d.) zirconia rotors with sample volume of 80 μL and spun at 12 kHz at RT. ^{13}C CPMAS spectra were recorded using a standard ramp cross-polarisation pulse sequence with contact times of 2-4 ms (^{13}C), a ^{1}H 90° pulse of 2.90 μs, recycle delays of 40-50 s and 198-1051 transients. Non-quaternary-suppression (NQS) experiments were performed with dephasing times of 45 μs and 180° ^{13}C refocusing pulse of 8 μs.

Carbon chemical shift scale was externally referenced via the resonance of glycine (^{13}C CH_2 signal at 43,86 ppm relative to tetramethylsilane).

Computational Details. Calculations were performed with the Gaussian 09 package[19] employing the density functional theory (DFT) method with Becke's three parameter hybrid functional and Lee-Yang-Parr's gradient-corrected correlation functional (B3LYP), with 6-311++G(d,p) as basis set. The geometries of the compounds were optimized in the gas phase and the nature of all stationary points was confirmed by a normal-mode analysis. Thermal correction based on harmonic vibrational frequencies and Gibbs free energy calculations were performed at 298.15 K and 1 atm. DFT calculations herein performed does not take into account the interactions in the melted state, which is beyond the scope of the present job, but the results appear to be reasonably in agreement with the experimental data. These geometries were employed to compute the absolute magnetic shielding σ, performed at the B3LYP/6-311++G(d,p) level

using the GIAO method of Gaussian 09, and the σ values were converted into ^{13}C chemical shifts δ relative to the magnetic shielding of TMS, taken as reference, computed at the same level (σ = –184.0724).

References

1) G. Rothenberg, A. P. Downie, C. L. Raston, J. L. Scott, *J. Am. Chem. Soc.* 2001, **123**, 8701–8708; G. W. V. Cave**;** C. L. Raston, J. L. Scott, *Chem. Commun.* 2001, 2159–2169; K. Tanaka, F. Toda, 2000, **100**, 1025–1074; J. Long, J. Hu,X.Shen, B. Ji, K. Ding, *J. Am. Chem. Soc.* 2002, **124**, 10–11; F. Toda, *Acc. Chem. Res*. 1995, **28**, 480–486; F. Toda, Synlett 1993, 303–312.

2) G. R. Desiraju, *Crystal Engineering: The Design of Organic Solids*, Elsevier, Amsterdam, 1989; M. D. Hollingsworth, *Science* 2002, **295**, 2410–2413; D. Braga, F. Grepioni, G. R. Desiraju, *Chem. Rev.* 1998, **98**, 1375–1405; D. Braga, G. R. Desiraju, J. Miller, A. G. Orpen, S. Price, *CrystEngComm* 2002, **4**, 500–509; D. Braga, L. Brammer, N. Champness, *CrystEngComm* 2005, **7**, 1–19.]

3) M. Ogawa, T. Hashizume, K. Kuroda, C. Kato, *Inorg. Chem.* 1991, **30**, 584–585; J. M. Thomas, R. Raja, G. Sankar, B. F. G. Johnson, D. W. Lewis, *Chem. Eur. J.* 2001, **7**, 2973– 2978; P. J. Nichols, C. L. Raston, J. W. Steed, *Chem. Commun.* 2001, 1062–1063; R. Kuroda, Y. Imal, T. Sato, *Chirality* 2001, **13**, 588–594; S. Apel, M. Lennartz, L. R. Nassimbeni, E. Weber, *Chem. Eur. J.* 2002, **8**, 3678–3686; L. R. Nassimbeni, *CrystEngComm* 2003, **5**, 200–203.

4) M. C. Etter, *J. Phys. Chem.* 1991, **95**, 4601–4610; M. C. Etter, S. M. Reutzel, C. G. Choo, *J. Am. Chem. Soc.* 1993, **115**, 4411–4412; W. H. Ojala, M. C. Etter, *J. Am. Chem. Soc.* 1992, **114**, 10228–10293; V. R. Pedireddi, W. Jones, A. P. Chorlton, R. Docherty, *Chem. Commun.* 1996, 987–988; A. V. Trask, W. D. S. Motherwell, W. Jones, *Chem. Commun.* 2004, 890–891.

5) D. Braga, M. Curzi, A. Johansson, M. Polito, K. Rubini, F. Grepioni, *Angew. Chem. Int. Ed.* 2006, **45**, 142–146; A. Pichon, A. Lazuen-Garay, S. L. James, *CrystEngComm* 2006, **8**, 211–214; D. Braga, S. L. Giaffreda, F. Grepioni, A. Pettersen, L. Maini, M. Curzi, M. Polito, *Dalton Trans.* 2006, 1249–1263.

6) D. Braga, M. Curzi, M. Lusi, F. Grepioni, *CrystEngComm* 2005, **7**, 276–278; A. V. Trask, D. A. Haynes, W. D. S. Motherwell, W. Jones, *Chem. Commun.* 2006, 51–53.]

7) F.Toda, K. Tanaka, *Chem. Rev.* 2000, **100**, 1025-1074.

8) J. Schmeyers, F. Toda, J. Boy, G. J. Kaupp, *J. Chem. Soc., Perkin Trans. 2* 1998, 989-993. F. Toda, M. Yagi, K. J. Kiyoshige, *Chem. Soc., Chem. Commun.* 1988, 958-959.

9) B. S. Goud, G. R. J. Desiraju, *Chem. Res., Synop.* 1995, 244-245; F. Toda, K. Tanaka, S. J. Iwata, *J. Org. Chem.* 1989, **54**, 3007-3009; F. Toda,; H. Takumi, A. J. Masafumi*, J. Chem. Soc., Chem. Commun.* 1990, 1270-1271; G. Kaupp, J. Schmeyers, A. Kuse, A. Atfeh, *Angew. Chem., Int. Ed.* 1999, **38**, 2896-2899; F. Toda, S. Tatsuya, *J. Chem. Soc., Perkin Trans. 1* 1989, 209-211; J. Im, J. Kim, S. Kim, B.Hahn, F. Toda, *Tetrahedron Lett.* 1996, **38**, 451-452.

10) G. Rothenberg, A. P. Downie, C. L. Raston, J. L. Scott, *J. Am.Chem. Soc.* 2001, **123**, 8701–8708.

11) D. Braga, S. L. Giaffreda, K. Rubini, F. Grepioni, M. R. Chierotti, R. Gobetto, *CrystEngComm* 2007, **9**, 39-45; V. P. Balema, J. W. Wiench, M. Pruski, V. K. Pecharsky, *Chem. Commun.* 2002, 724-725.

12) G. Kaupp, *CrystEngComm* 2003, **5**, 117–133.

13) *Solid State Chemistry Techniques* , Ed.: A. K. Cheetham, Oxford University Press, Oxford, 1987.

14) M. Shiri, M. A. Zolfigol, H. G. Kruger, Z. Tanbakouchian, *Chem. Rev.* 2010, **110**, 2250 and references therein~~)~~.

15) M. Barbero, S. Cadamuro, S. Dughera, C. Magistris, P. Venturello, *Org. Biomol. Chem.* 2011, **9**, 8393~~)~~.

16) J. F. Stebbins, I. Farnan, N. Dando,; S. Y. Tzeng, *J. Am. Ceram. Soc.* 1992, **75**, 3001-3006; E. Robert; V. Lacassagne, C. Bessada, D. Massiot, B. Gilbert, J.-P. Coutures, *Inorg. Chem.* **1999**, *38*, 214-217; c) V. Lacassagne, C. Bessada, P. Florian, S. Bouvet, B. Ollivier, J.-P. Coutures, D. Massiot, *J. Phys. Chem. B* 2002, **106**, 1862-1868; I. Nuta, E.Veron, G. Matzen, C. Bessada, *Inorg. Chem.* 2011, **50,** 3304-3312].

17) G. Rothenberg, P. A. Downie, C. L. Raston, J. L. Scott, *J. Am. Chem. Soc.* 2001, **123**, 8701-8708; R. Hiraoka, H. Watanabe, M. Senna *Tetrahedron Letters* 2006, **47**, 3111–3114.]

18) G. A. Olah, *J. Org. Chem.* 2001, **66**, 5943.

19) M. J. Frisch, G. W. Trucks, H. B. Schlegel, G. E. Scuseria, M. A. Robb, J. R. Cheeseman, G. Scalmani, V. Barone, B. Mennucci, G. A. Petersson, H. Nakatsuji, M. Caricato, X. Li, H. P. Hratchian, A. F. Izmaylov, J. Bloino, G. Zheng, J. L. Sonnenberg, M. Hada, M. Ehara, K. Toyota, R. Fukuda, J. Hasegawa, M. Ishida, T. Nakajima, Y. Honda, O. Kitao, H. Nakai, T. Vreven, J. A. Jr. Montgomery, J. R. Peralta, F. Ogliaro, M. Bearpark, J. J. Heyd, E. Brothers, K. N. Kudin, V. N. Staroverov, R. Kobayashi, J. Normand, K. Raghavachari, A. Rendell, J. C. Burant, S. S. Iyengar, J. Tomasi, M. Cossi, N. Rega, J. Millam, M. Klene, J. E. Knox, J. B. Cross, V. Bakken, C. Adamo, J. Jaramillo, R. Gomperts, R. E. Stratmann, O. Yazyev, A. J. Austin, R. Cammi, C. Pomelli, J.

Ochterski, R. L. Martin, K. Morokuma, V. G. Zakrzewski, G. A. Voth, P. Salvador, J. J. Dannenberg, S. Dapprich, A. D. Daniels, O. Farkas, J. B. Foresman, J. V. Ortiz, J. Cioslowski, D. J. Fox, *Gaussian 09, Rev. A.02,* 2009, Wallingford CT, Gaussian, Inc.

Figures and Schemes

a b c d e

Figure 1. a) powdered samples: **1**^{A} (right) and **2** (left); b) powdered **1**^{A} and **2** mixed at room temperature; c) immediately after reagent contact, an orange liquid phase forms at the contact surface; d) after merely mixing with a glass rod the entire mass becomes a homogeneous liquid melted phase; e) the solid, yellow final product **5**^{A}**.**

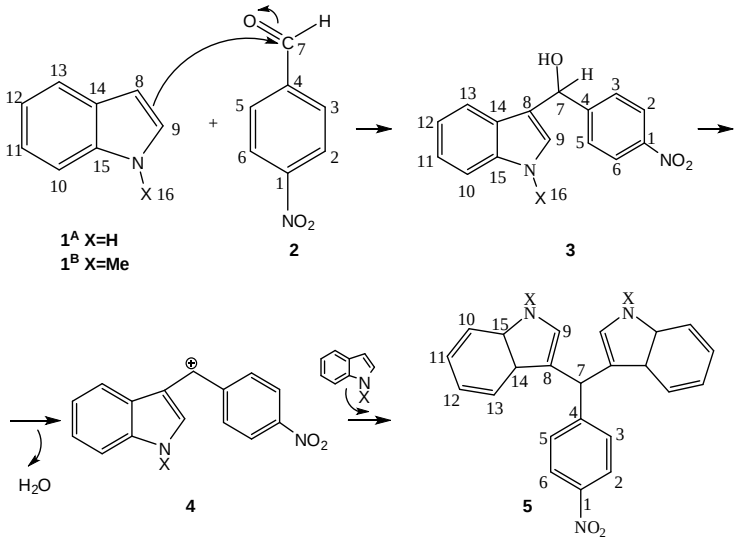

Scheme 1

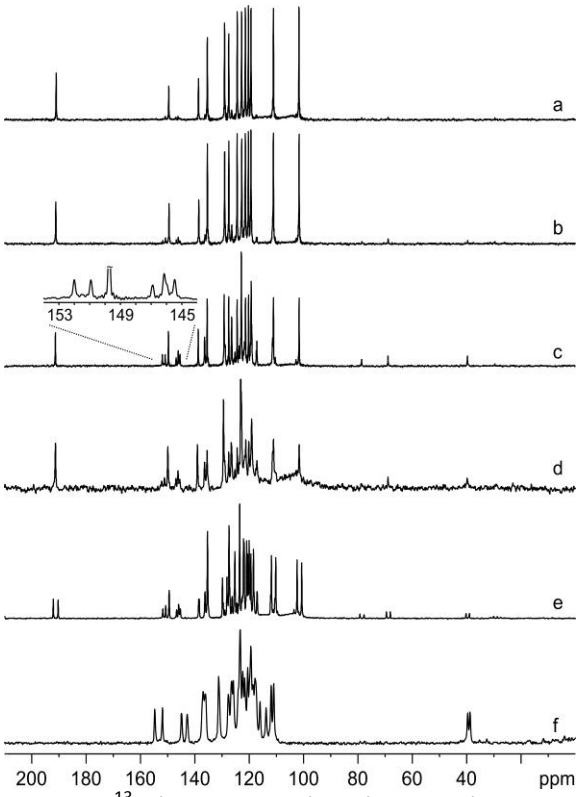

Figure 2. ^{13}C (100.64 MHz) DE (a, b, c, d), DE without proton decoupling (e) and CPMAS (f) spectra of the reaction between **1**^{A} and **2** at: a) t=0, spectrum of reagents in the melted phase; b) t=2h, signals of **3**^{A}, of a hydrogen-bonded intermediate and of **5**^{A} start appearing; c) t=7h, the signals of **3**^{A}, of a hydrogen-bonded intermediate and of the product grow; d) t=13h, noisy spectrum due to product precipitation and reagent consuming; e) t=7h; f) solid yellow product **5**^{A}. All spectra were recorded with a spinning speed of 12 kHz at RT.

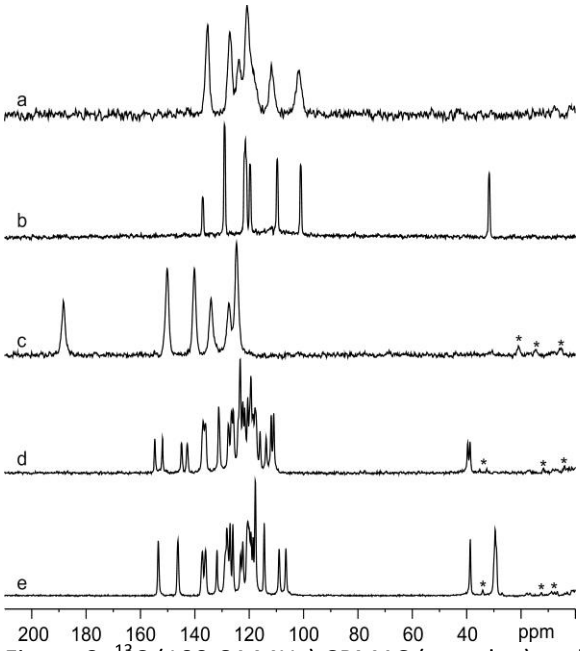

Figure 3: ^{13}C (100.64 MHz) CPMAS (a, c, d, e) and DE (b) experiments of pure a) indole (**1**^{A}), b) N-methylindole (**1**^{B}), c) 4-nitrobenzladehyde (**2**), d) final product **5**^{A} and e) final product **5**^{B} recorded at with a spinning speed of 12 kHz at RT. Asterisks denote spinning sidebands.

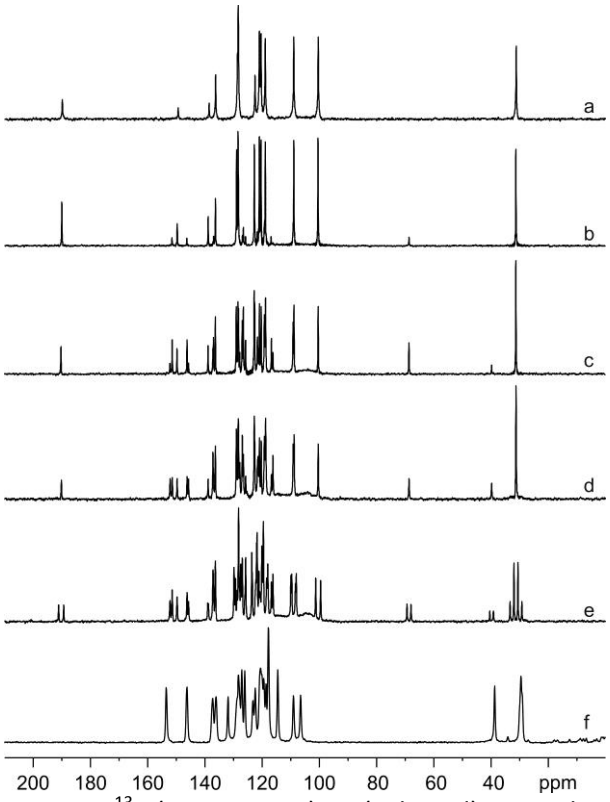

Figure 4: ^{13}C (100.64 MHz) DE (a, b, c, d), DE without decoupling (e) and CPMAS (f) spectra of the reaction between $\mathbf{1}^{\mathbf{B}}$ and **2** at: a) t=0, spectrum of reagents in the melted phase; b) t=9h, signals of $\mathbf{3}^{\mathbf{B}}$ appears; c) t=11h, the signals of $\mathbf{3}^{\mathbf{B}}$ grow while signals of $\mathbf{5}^{\mathbf{B}}$ start appearing; d) t=13h, the signals of $\mathbf{3}^{\mathbf{B}}$ start decreasing; e) t=13h; f) solid yellow product $\mathbf{5}^{\mathbf{B}}$. All spectra were recorded with a spinning speed of 12 kHz and at RT.

Table 1[a] ^{13}C chemical shift assignments for pure solid compounds **1**^{A}, **2**, **5**^{A} and **5**^{B}, and pure liquid **1**^{B}.

atom	**1**^{A}	**1**^{B}	**2**	**5**^{A} **solid**	**5**^{B} **solid**
C1			150.1	144.8/142.7	146.2
C2			124.6	123.3 - 110.9	128.1
C3			133.8	136.1/131.2	128.7sh
C4			140.1	154.7/151.9	153.4
C5			127.4	136.1	131.8
C6			124.6	123.3 - 110.9	128.1
C7			188.3	39.7/38.9	38.8
C8	101.6	101.1		119.4sh/117.6/116.0/113.7	114.7/114.4
C9	123.6	121.4		123.3 - 110.9	106.5 - 123.1
C10	111.7	109.6			
C11	118.3	119.6			
C12	120.6	121.4			
C13					
C14	127.0	129.1		127.6/126.5/125.8	127.0/126.6
C15	135.1	137.0		131.2	137.1/136.0
C16		31.7			29.6/29.2

[a] for atom labeling we refer to scheme 1.

Table 2[a] Experimental and calculated (only for the indole reaction) ^{13}C chemical shifts with assignment of compounds **1**^{A}, **1**^{B}, **2**, **5**^{A} and **5**^{B} in the melt.

atom	1^A exp	1^A calc	1^B exp	2^A exp	2^A calc	2^B exp	3^A exp	3^A calc	3^Bexp	5^A exp	5^A calc	5^B exp
C1				149.6	158.7	149.3	146.1	155.4	146.3	145.5	154.7	145.7
C2				124.5	130.9	128.6/		130.4	126.5		130.9 (130.7)	
C3				129.1	139.8	128.3		133.0	126.5		135.2 (136.3)	
C4				138.7	146.4	138.5	150.9	160.4	151.5	152	162.7	152.1
C5				127.6	133.9	128.6/		133.2	128.7		136.3 (135.2)	
C6				124.5	131.2	128.3		129.4	126.5		130.7 (130.9)	
C7				191.0	195.6	189.7	68.9	73.5	68.6	39.7	43.5	39.8
C8	101.8	108.9	100.4					130.5	125.8		128.6 (125.5)	122.3sh
C9	121.5	127.8	121.0					129.2	121.6		129.2 (130.6)	121.4
C10	111.2	114.8	108.9					115.8	109.2		115.1 (115.0)	109.2
C11	122.8	127.9	122.4					129.5	119,1/		128.9 (128.3)	
C12	119.5	125.8	118.9					127.3	116,9		126.0 (126.2)	119.2/
C13	120.4	126.6	120.4					122.8			125.4 (125.1)	116.2
C14	135.5	135.9	136.2					133.8	126.8		134.6 (134.4)	127.8
C15		143.0						142.9	136.9		143.6 (143.8)	137.2
C16			31.2						31.3			

[a] only signals whose assignment is certain are reported